Controlling purity, indistinguishability, and quantum yield of an incoherently pumped two-level system by spectral filters

Ivan V. Panyukov
Moscow Institute of Physics and Technology, 9 Institutskiy Pereulok, Dolgoprudny 141700, Moscow Region, Russia and Dukhov Research Institute of Automatics (VNIIA), 22 Sushchevskaya, Moscow 127055, Russia

Vladislav Yu. Shishkov* and Evgeny S. Andrianov
Dukhov Research Institute of Automatics (VNIIA), 22 Sushchevskaya, Moscow 127055, Russia; Moscow Institute of Physics and Technology, 9 Institutskiy Pereulok, Dolgoprudny 141700, Moscow Region, Russia; Center for Photonics and Quantum Materials, Skolkovo Institute of Science and Technology, Moscow 121205, Russia; and Laboratories for Hybrid Photonics, Skolkovo Institute of Science and Technology, Moscow 121205, Russia

(Received 19 December 2022; accepted 21 July 2023; published 10 August 2023)

Dephasing processes significantly impact the performance of deterministic single-photon sources. Dephasing broadens the spectral line and suppresses the indistinguishability of the emitted photons, which is undesirable for many applications, primarily for quantum computing. We consider a light emitted by a two-level system with a pulsed incoherent pump in the presence of the spectral filter. The spectral filter allows control of the second-order autocorrelation function, indistinguishability, and quantum yield. We show that narrow spectral filters can increase the indistinguishability of the emitted light while undermining the quantum yield. The influence of the spectral filter on the second-order autocorrelation function depends on the duration of the pump. When the pump pulse is long compared to the lifetime of the two-level system, the narrow spectral filters lead to a rapid increase in the second-order autocorrelation function. In this limit, the statistics of the light from the two-level system inherit the statistics of the incoherent pump. In the case of the short duration of the pump pulse, it is possible to preserve single-photon properties to some degree for the sublifetime width of the spectral filter. Moreover, the single-photon properties of the light manifest themselves differently, depending on the response time of the quantum system affected by this light. In particular, in the case of long response time, the spectral filter with a sublifetime width can provide the near-zero second-order autocorrelation function.

DOI: 10.1103/PhysRevA.108.023711

I. INTRODUCTION

Single-photon sources (SPSs) have a wide range of applications, including quantum cryptography [1–3], quantum communication [4,5], quantum computing [6–9], quantum metrology [10,11], and quantum information processing [12,13], and are compatible with integral nanophotonics [14,15].

Three metrics characterize the SPS's performance: quantum yield, indistinguishability, and second-order autocorrelation function (purity). The quantum yield stands for the probability of the photon emission of the SPS. Indistinguishability indicates the ability of the emitted photons to interfere. The measurement of the indistinguishability requires the Hong-Ou-Mandel setup [16–19]. The second-order autocorrelation function determines the fluctuations of the radiation intensity and statistics of the emitted light. Generally, the second-order autocorrelation function is equal to or greater than zero. If an SPS emits only one photon at a time, the second-order autocorrelation function is zero. While some applications of SPSs, such as quantum cryptography, require only a low second-order autocorrelation function, most applications of SPSs require appropriate values of all the above-described parameters simultaneously.

Quantum dots, silicon-vacancy (SiV) centers, nitrogen-vacancy (NV) centers, and single molecules serve as SPSs operating at room temperature. However, these systems have high dephasing rates [20–22], and, therefore, the indistinguishability of the emitted photons is low. Indeed, according to Ref. [23], the indistinguishability of photons emitted by SPSs is equal to $I = \gamma_{\text{diss}}/(\gamma_{\text{diss}} + \gamma_{\text{deph}})$, where γ_{diss} and γ_{deph} are the rates of dissipation and dephasing, respectively. For quantum dots, SiV centers, and NV centers, γ_{deph} can be as high as $10^5\gamma_{\text{diss}}$ at room temperature [24], which results in low indistinguishability.

Several approaches to increase indistinguishability have emerged in recent years. One approach is to lower the temperature of the SPS, decreasing γ_{deph} [25,26]. Another approach is to place the photon emitter near a cavity, increasing γ_{diss} [20,24,27–32]. The achievement of high values of indistinguishability usually requires the combination of these two methods [33]. The spectral filters can increase the indistinguishability of photons emitted by an SPS [34]. However, this method decreases the quantum yield. In addition, it is unknown how the spectral filter affects the

*vladislavmipt@gmail.com

second-order autocorrelation function for an SPS with a pulsed incoherent pumping.

Many experimental setups incorporate laser for incoherent or coherent pumping of SPSs [30,35–39]. However, electrically driven single-photon sources are preferable for a mass-production of single-photon sources for applications in quantum information technology [40,41]. The electrical excitation of the single-photon sources corresponds to the incoherent pumping [42–47].

In this paper, we consider a two-level system (TLS) with pulsed incoherent pumping as an SPS. We investigate the effect of spectral filtering on the light emitted by an SPS. The spectral filters affect the quantum yield, the indistinguishability, and the second-order autocorrelation function. The sublifetime spectral filters provide high indistinguishability. However, the narrow spectral filter to the light emitted by the TLS leads to different second-order autocorrelation functions depending on the duration of the pump pulse. When the pumping duration exceeds the lifetime of an SPS, the second-order autocorrelation function is approximately two for narrow filters. At the short duration of the pump, a second-order autocorrelation function is low (from 1/5 to 2/3) for narrow spectral filters. We also show that the statistics of the light emitted by the SPS manifests itself nontrivially depending on the response time of the quantum system affected by this light.

II. MODEL DESCRIPTION

We consider a TLS as an SPS. The TLS is coupled to an environment responsible for relaxation processes in the TLS and its pumping. A full Hamiltonian is the sum of the Hamiltonians of the TLS, $\hat{H}_S$, the reservoirs, $\hat{H}_E$, and the interaction between the system and the reservoirs, $\hat{H}_{SE}$,

$$\hat{H} = \hat{H}_S + \hat{H}_E + \hat{H}_{SE}. \tag{1}$$

The Hamiltonian of the TLS is

$$\hat{H}_S = \hbar\omega_0 \hat{\sigma}^\dagger \hat{\sigma}, \tag{2}$$

where ω_0 is the transition frequency, and $\hat{\sigma} = |g\rangle\langle e|$, with the ground state and the excited state of the TLS being $|g\rangle$ and $|e\rangle$. Below we also refer to the state $|e\rangle$ as the working level of the SPS. The term $\hat{H}_E$ is the Hamiltonian of the environment:

$$\hat{H}_E = \sum_k \hbar\omega_{1k}\hat{\sigma}_k^\dagger\hat{\sigma}_k + \sum_k \hbar\omega_{2k}\hat{a}_{rk}^\dagger\hat{a}_{rk} + \sum_k \hbar\omega_{3k}\hat{a}_{nrk}^\dagger\hat{a}_{nrk} + \sum_k \hbar\omega_{4k}\hat{b}_k^\dagger\hat{b}_k, \tag{3}$$

where the terms on the right-hand side stand for reservoirs responsible for the incoherent pumping, the radiative energy dissipation, the nonradiative energy dissipation, and the dephasing, respectively. The reservoir of the incoherent pumping consists of two-level systems at an effective negative temperature [48]; the corresponding reservoir operators are $\hat{\sigma}_k = |g_k\rangle\langle e_k|$, where $|g_k\rangle$ and $|e_k\rangle$ are the ground state and the excited state of the TLS with the number k, and ω_{1k} is its transition frequency. The reservoirs responsible for radiative and nonradiative energy dissipation and dephasing are harmonic oscillators, with frequencies ω_{2k}, ω_{3k}, and ω_{4k} and annihilation operators $\hat{a}_{rk}$, $\hat{a}_{nrk}$, and $\hat{b}_k$, respectively. We note, that $\hat{a}_{rk}$ represent the annihilation operators of the electromagnetic modes. The Hamiltonian of the interaction between the TLS and the environment is

$$\hat{H}_{SE} = \sum_k \hbar g_{1k}(\hat{\sigma}_k^\dagger\hat{\sigma} + \hat{\sigma}_k\hat{\sigma}^\dagger)\theta(t)\theta(T-t) + \sum_k \hbar g_{2k}(\hat{a}_{rk}^\dagger\hat{\sigma} + \hat{a}_{rk}\hat{\sigma}^\dagger) + \sum_k \hbar g_{3k}(\hat{a}_{nrk}^\dagger\hat{\sigma} + \hat{a}_{nrk}\hat{\sigma}^\dagger) + \sum_k \hbar g_{4k}\hat{\sigma}^\dagger\hat{\sigma}(\hat{b}_k^\dagger + \hat{b}_k), \tag{4}$$

where g_{1k}, g_{2k}, g_{3k}, and g_{4k} are the interaction constants of the TLS with the corresponding reservoirs. Theta functions in the first term mean that the interaction between the TLS and the incoherent pumping reservoir exists at $0 \leqslant t \leqslant T$. We assume that the temperatures of the dissipation reservoirs are much lower than $\hbar\omega_0/k_B$, which is a good assumption if ω_0 is an optical or near-infrared spectral range. Next, using the Born-Markov approximation, we eliminate degrees of freedom of the environment to obtain an equation for the density matrix of the TLS. As a result, we obtain the Lindblad equation on the density matrix $\hat{\rho}$ of the TLS [48,49] as

$$\frac{\partial\hat{\rho}}{\partial t} = -\frac{i}{\hbar}[\hat{H}_S, \hat{\rho}] + L_{\text{pump}}[\hat{\rho}] + L_{\text{diss}}[\hat{\rho}] + L_{\text{deph}}[\hat{\rho}], \tag{5}$$

where the relaxation operators $L_{\text{pump}}[\hat{\rho}]$, $L_{\text{diss}}[\hat{\rho}]$, and $L_{\text{deph}}[\hat{\rho}]$ describe the incoherent pumping, the energy dissipation, and the dephasing with the corresponding rates γ_{pump}, γ_{diss}, and γ_{deph} as follows:

$$L_{\text{pump}}[\hat{\rho}] = \frac{\gamma_{\text{pump}}(t)}{2}(2\hat{\sigma}^\dagger\hat{\rho}\hat{\sigma} - \hat{\sigma}\hat{\sigma}^\dagger\hat{\rho} - \hat{\rho}\hat{\sigma}\hat{\sigma}^\dagger), \tag{6}$$

$$L_{\text{diss}}[\hat{\rho}] = \frac{\gamma_{\text{diss}}}{2}(2\hat{\sigma}\hat{\rho}\hat{\sigma}^\dagger - \hat{\sigma}^\dagger\hat{\sigma}\hat{\rho} - \hat{\rho}\hat{\sigma}^\dagger\hat{\sigma}), \tag{7}$$

$$L_{\text{deph}}[\hat{\rho}] = \frac{\gamma_{\text{deph}}}{2}(2\hat{\sigma}^\dagger\hat{\sigma}\hat{\rho}\hat{\sigma}^\dagger\hat{\sigma} - \hat{\sigma}^\dagger\hat{\sigma}\hat{\rho} - \hat{\rho}\hat{\sigma}^\dagger\hat{\sigma}). \tag{8}$$

We assume that until $t = 0$ TLS is in the ground state. At the moment $t = 0$, incoherent pumping begins to act on the TLS. The incoherent pumping starts at $t = 0$, then remains constant, and terminates at $t = T$, i.e., $\gamma_{\text{pump}}(t)$ in Eq. (6) equals $\gamma_{\text{pump}} \neq 0$ at $0 \leqslant t \leqslant T$, and is zero at other times. In the incoherent pumping scheme, the initial pulse excites electrons to the levels of the SPS higher than the working level. The electrons on these levels are sometimes called hot electrons. The initial excitation then transits to the working level of the SPS [36]. Equation (6) describes this process as an effective transition from the ground state to the working level of an SPS. This model is valid for quantum dots [50–55], single molecules [56,57], NV centers and SiV centers [13,58–62], and two-dimensional materials [63,64]. In general, the duration of the incoherent pumping, T, is the sum of two times: the pumping duration and the relaxation time from the higher levels of the SPS to the working level. The latter time determines the lower bound of T and may vary depending on the physical realization of the SPS. For instance, in quantum dots the characteristic ratio between γ_{diss} and the relaxation rate of hot electrons towards the working level ranges from 10^2 to 10^4 [65–71]. Below we refer to the time T as the pump-pulse duration and mind its lower bound.

At $0 \leqslant t \leqslant T$ the relaxation rate of the population of the TLS, γ (longitudinal relaxation), and the relaxation rate of the dipole moment of the TLS, Γ (transverse relaxation), depend on both dissipation and pumping processes and can be found from the master equation (5) [48,72]:

$$\gamma = \gamma_{\text{pump}} + \gamma_{\text{diss}}, \tag{9}$$

$$\Gamma = \frac{\gamma_{\text{pump}} + \gamma_{\text{diss}} + \gamma_{\text{deph}}}{2}. \tag{10}$$

The physical reason for dephasing is the interaction between electrons and phonons. In this paper, we consider the phonons in the Markovian approximation.

The metrics of SPS can be obtained from the annihilation operator of the electric field at the detector $\hat{E}(t)$ in the Heisenberg representation. The dipole moment operator of the TLS $\hat{\mathbf{d}}$ is related to $\hat{\sigma}$ as $\hat{\mathbf{d}} = \mathbf{d}_{eg}(\hat{\sigma} + \hat{\sigma}^\dagger)$ [73], where $\mathbf{d}_{eg}$ is the matrix element of the dipole transition between the ground state and the excited state. Thus, $\hat{\sigma}$ is the dimensionless dipole moment operator. Therefore, for the light emitted by an SPS,

$$\hat{E}(t) \propto \hat{\sigma}(t - r/c), \tag{11}$$

where r is the distance from the SPS to the detector [74]. Hereafter we neglect the propagation time r/c. From Eq. (11) it follows that correlations of the electromagnetic field are connected to the correlations of TLS operators $\hat{\sigma}(t)$. Thus, multitime correlations $\langle \hat{\sigma}^\dagger(t_1)\hat{\sigma}(t_2)\rangle$ and $\langle \hat{\sigma}^\dagger(t_1)\hat{\sigma}^\dagger(t_2)\hat{\sigma}(t_3)\hat{\sigma}(t_4)\rangle$ can be obtained from Lindblad equation (5) and, as we show below, can be used to determine the indistinguishability and purity of the emitted light.

A complex transmission function $F(\omega)$ completely characterizes a spectral filter. The filter acts on the light by multiplying the Fourier component of the electric field with the frequency ω by $F(\omega)$. Thus, in the presence of a spectral filter, the parameters of an SPS are determined by the filtered electric field

$$\hat{E}_F(t) = \int_{-\infty}^{+\infty} \frac{d\omega}{2\pi} F(\omega) \int_{-\infty}^{+\infty} dt' \hat{E}(t') e^{-i\omega(t-t')}. \tag{12}$$

The interaction mechanism between the light and the filter is described in detail in Ref. [75]. Regardless of the particular implementation of the spectral filter, the causality principle for the transmitted light should be satisfied. This implies the fulfillment of the Kramers-Kronig relation for $F(\omega)$. Therefore, we can introduce the transfer function

$$f(\Delta t) = \int_{-\infty}^{+\infty} F(\omega) e^{-i\omega\Delta t} \frac{d\omega}{2\pi} \tag{13}$$

and express $\hat{E}_F(t)$ as

$$\hat{E}_F(t) = \int_{-\infty}^{t} f(t - t')\hat{E}(t')dt'. \tag{14}$$

Below, we consider a Lorentz spectral filter:

$$F(\omega) = \frac{\gamma_F}{\omega - \omega_F + i\gamma_F}. \tag{15}$$

Here ω_F is the central frequency of the filter, which stands for the maximum of $|F(\omega)|^2$, and γ_F represents the width of this maximum. The normalization $|F(\omega_F)| = 1$ means that the filter transmits all the light at the frequency, ω_F. Hereafter, we assume that the filter transmits all the light at the transition frequency of the TLS, $\omega_F = \omega_0$.

III. INDISTINGUISHABILITY

The indistinguishability of the photons determines their ability to interfere. In the case of a spectral filter, the indistinguishability is [76]

$$I_F = \frac{\int_{-\infty}^{+\infty} dt_1 \int_{-\infty}^{+\infty} dt_2 |\langle \hat{E}_F^\dagger(t_1)\hat{E}_F(t_2)\rangle|^2}{(\int_{-\infty}^{+\infty} dt \langle \hat{E}_F^\dagger(t)\hat{E}_F(t)\rangle)^2}. \tag{16}$$

We present I_F explicitly in terms of operators $\hat{\sigma}$ and $\hat{\sigma}^\dagger$ in Appendix A. The calculation I_F requires $\langle \hat{\sigma}^\dagger(t_1)\hat{\sigma}(t_2)\rangle$. Equation (5) allows calculating this correlator via the quantum regression theorem [49].

In the absence of a filter the indistinguishability can be obtained according to

$$I_F|_{\text{no filter}} = I_0 \frac{2(T\gamma_{\text{diss}} + e^{-T\gamma_{\text{diss}}} - 1)}{T^2\gamma_{\text{diss}}^2}. \tag{17}$$

where

$$I_0 = \frac{\gamma_{\text{diss}}}{\gamma_{\text{diss}} + \gamma_{\text{deph}}}. \tag{18}$$

One can see that $I_F|_{\text{no filter}} \to I_0$ as $T \to 0$, which agrees with the results obtained in Ref. [23].

Figure 1 shows the dependence of the indistinguishability I_F on two parameters: the filter width and the duration of the pump pulse. At small pump-pulse duration ($T < \gamma_{\text{diss}}^{-1}$), high indistinguishability is observed for a wider range of filter widths, γ_F. In this case, the indistinguishability increases from $\gamma_{\text{diss}}/(\gamma_{\text{diss}} + \gamma_{\text{deph}})$ to 1, as the filter width decreases. Therefore, spectral filtering increases indistinguishability.

The analytical expression for the indistinguishability in the presence of the spectral filter is lengthy. Therefore, we consider in detail only some limiting cases.

In the case of a wide spectral filter, $\gamma_F \gg \gamma_{\text{deph}}$, we obtain $I_F \approx I_F|_{\text{no filter}}$. The indistinguishability is low at $\gamma_{\text{deph}} \gg \gamma_{\text{diss}}$ and with a wide spectral filter see Eq. (17). However, the spectral filter and the short pump pulse can significantly increase indistinguishability. Indeed, in the case $T \ll \max\{\gamma_{\text{diss}}^{-1}, (\gamma_{\text{diss}}\gamma_{\text{deph}})^{-1/2}, (\gamma_{\text{diss}}\gamma_F)^{-1/2}\}$, we obtain

$$I_F \approx I_0 \Bigg(1 + \frac{\gamma_{\text{deph}}}{\gamma_{\text{diss}} + 2\gamma_F} \cdot \frac{\gamma_{\text{deph}} + 3\gamma_{\text{diss}} + 4\gamma_F}{\gamma_{\text{deph}} + 3\gamma_{\text{diss}} + 2\gamma_F} - \frac{T^2\gamma_F\gamma_{\text{diss}}}{12} \cdot \frac{\gamma_{\text{diss}} + \gamma_{\text{deph}} + 2\gamma_F}{\gamma_{\text{diss}} + 2\gamma_F} \cdot \frac{2\gamma_{\text{deph}} + 3\gamma_{\text{diss}} + 2\gamma_F}{\gamma_{\text{deph}} + 3\gamma_{\text{diss}} + 2\gamma_F}\Bigg). \tag{19}$$

Moreover, the fulfillment of the conditions $\gamma_F \ll \gamma_{\text{diss}}$ and $T \ll (\gamma_{\text{diss}}\gamma_F)^{-1/2}$ makes the indistinguishability of an SPS close to unity:

$$I_F \approx 1 - 2\frac{\gamma_F}{\gamma_{\text{diss}}} - T^2\frac{\gamma_{\text{diss}}\gamma_F}{6}. \tag{20}$$

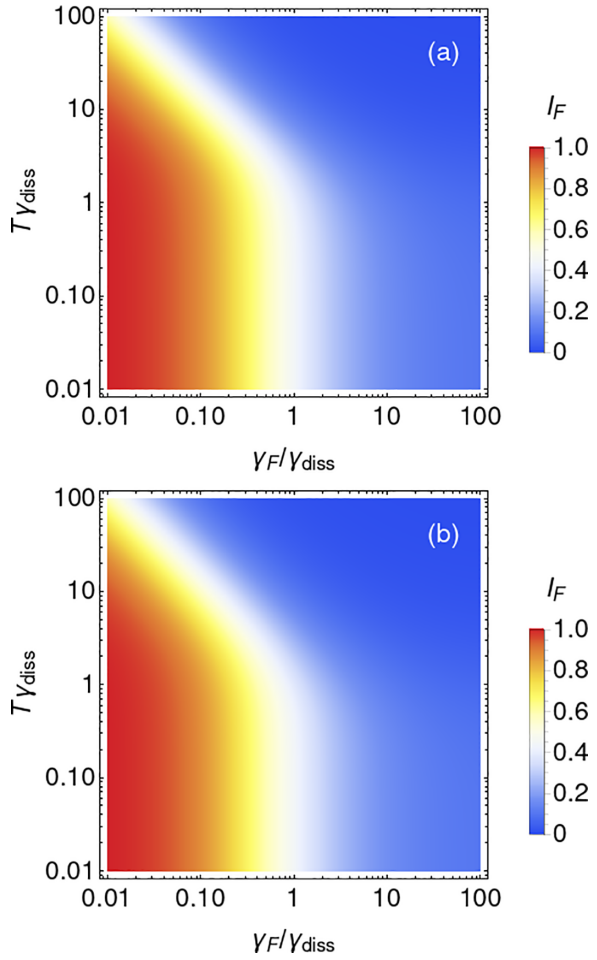

FIG. 1. The dependence of the indistinguishability I_F on the filter width γ_F and the pump-pulse duration T in the case of $\gamma_{\rm deph} = 10\gamma_{\rm diss}$ if (a) $\gamma_{\rm pump} = 0.01\gamma_{\rm diss}$ and (b) $\gamma_{\rm pump} = 5\gamma_{\rm diss}$.

Let us discuss the experimental feasibility of high indistinguishability at a high dephasing rate due to spectral filtering. In particular, we consider the region $T\gamma_{\rm diss} < 1$ and $\gamma_F < 0.1\gamma_{\rm diss}$ on Fig. 1. The typical lifetime of molecules or quantum dots is on the order of a nanosecond. The corresponding pump-pulse duration T should be about a tenth of a nanosecond. This is easily achievable with both optical and electrical pumping [40], given the hot electron dynamics are fast [65–71]. The condition $\gamma_F < 0.1\gamma_{\rm diss}$ means that the width of the bandpass filter should correspond to γ_F^{-1}, which is more than a dozen nanoseconds. For filters based on resonators, this condition implies the required Q factor is of an order of 10^8. This can be achieved, e.g., in an on-chip Si_3N_4 resonator with a Q factor greater than 1×10^9 at telecom wavelength [77]. The single-photon light sources at telecom wavelengths are also available [35,45,78,79]. An InAs/GaAs quantum dot emitting at telecom wavelengths with the dissipation time around 1 ns and the total dephasing time around 100 ps was reported in Ref. [80]. Moreover, an InAs/GaAs electrically pumped quantum dot with a 1-ns lifetime was demonstrated [40]. Thus, we suggest that high indistinguishability due to spectral filtering at a high dephasing rate of a single-photon source is experimentally achievable. This analysis is also relevant to the following sections.

IV. SECOND-ORDER AUTOCORRELATION FUNCTION

The second-order autocorrelation function $g^{(2)}(t,0) = \frac{\langle \hat{E}^\dagger(t)\hat{E}^\dagger(t)\hat{E}(t)\hat{E}(t)\rangle}{\langle \hat{E}^\dagger(t)\hat{E}(t)\rangle^2}$, in the presence of the spectral filter, changes to

$$g_F^{(2)}(t,0) = \frac{\langle \hat{E}_F^\dagger(t)\hat{E}_F^\dagger(t)\hat{E}_F(t)\hat{E}_F(t)\rangle}{\langle \hat{E}_F^\dagger(t)\hat{E}_F(t)\rangle^2}. \tag{21}$$

This definition implies that the detector registers the light instantaneously [81].

If the response time of the detector, τ, is finite, the measured second-order autocorrelation function may differ from the expression (21). We can neglect the finiteness of the response time of the detector and use Eq. (21) as long as $\tau \ll \tau_{\rm TLS}$, where $\tau_{\rm TLS}$ is the emission time of the SPS, $\tau_{\rm TLS} \sim T + 1/\gamma_{\rm diss}$. Below, we consider single-photon properties of the light in two limiting cases: $\tau \gg \tau_{\rm TLS}$ and $\tau \ll \tau_{\rm TLS}$. When $\tau \gg \tau_{\rm TLS}$ we consider two distinct situations: when τ is the duration of the photoelectric effect process which is equal to the exposition time and when the τ is the exposure time neglecting the duration of the photoeffect process. The latter case is closer to the experimental setups. For example, the exposition time of the electron-multiplying charge-coupled device (EMCCD) camera is of the order of milliseconds and the photoeffect processes are instantaneous [82,83].

A. Short detector response time

Detection is almost instantaneous in the case $\tau \ll \tau_{\rm TLS}$. We denote the time at which detection occurs as t. We limit ourselves to the case $t = T$, corresponding to the moment in time when the probability of light emission reaches the maximum. Thus, we consider $g_F^{(2)}(t,0)$ at the moment $t = T$.

We express $g_F^{(2)}(T,0)$ in terms of operators $\hat{\sigma}$ and $\hat{\sigma}^\dagger$ in Appendix A. To obtain $g_F^{(2)}(T,0)$, it is necessary to calculate the correlation functions $\langle \hat{\sigma}^\dagger(t_1)\hat{\sigma}^\dagger(t_2)\hat{\sigma}(t_3)\hat{\sigma}(t_4)\rangle$ and $\langle \hat{\sigma}^\dagger(t_1)\hat{\sigma}(t_2)\rangle$ for all possible relations between the times $\{t_1,t_2,t_3,t_4\}$. The correlation $\langle \hat{\sigma}^\dagger(t_1)\hat{\sigma}(t_2)\rangle$ and the correlation $\langle \hat{\sigma}^\dagger(t_1)\hat{\sigma}^\dagger(t_2)\hat{\sigma}(t_3)\hat{\sigma}(t_4)\rangle$ for normally ordered times $\{t_1,t_2,t_3,t_4\}$ can be obtained via the standard quantum regression theorem [48], using the master equation (5). In all other cases, the calculation of $\langle \hat{\sigma}^\dagger(t_1)\hat{\sigma}^\dagger(t_2)\hat{\sigma}(t_3)\hat{\sigma}(t_4)\rangle$ requires the generalized quantum regression theorem that was developed in Ref. [84]. The details of calculations are in Appendix C.

In the absence of the spectral filter, the second-order autocorrelation function for the light emitted by the TLS is zero:

$$g_F^{(2)}(T,0)|_{\rm no\ filter} = 0. \tag{22}$$

Figure 2 shows the dependence of $g_F^{(2)}(T,0)$ on two parameters: the width of the filter, γ_F, and the duration of the pump pulse, T. At $T \gg \gamma_{\rm diss}^{-1}$, a monotonous decrease of $g_F^{(2)}(T,0)$ from 2 to 0 is followed by the narrowing of the spectral filter. This case corresponds to the cw-pumping regime [85];

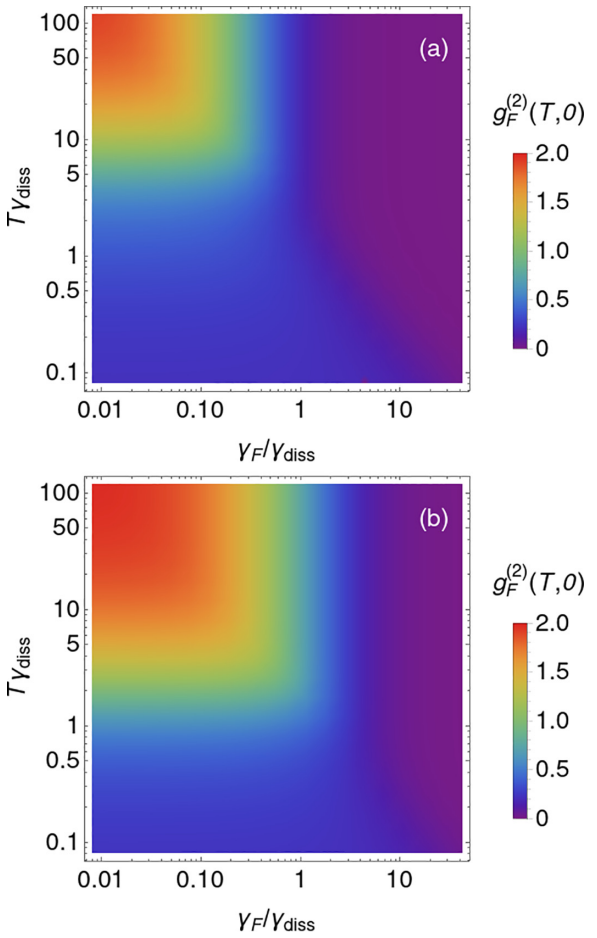

FIG. 2. The dependence of $g_F^{(2)}(T,0)$ on the filter width γ_F and the pump-pulse duration T at $\gamma_{\rm deph} = 10\gamma_{\rm diss}$ in the case of (a) $\gamma_{\rm pump} = 0.01\gamma_{\rm diss}$ and (b) $\gamma_{\rm pump} = 5\gamma_{\rm diss}$.

therefore, for $T \gg \gamma_{\rm diss}^{-1}$,

$$g_F^{(2)}(T,0) \approx \frac{2\gamma^2(\gamma_F+\gamma(1-2p)^2)(\Gamma+\gamma_F)}{(\gamma+2\gamma_F)\big(3\gamma\gamma_F+2\gamma_F^2+\gamma^2(1-2p)^2\big)(\Gamma+3\gamma_F)}, \tag{23}$$

where $p = \gamma_{\rm pump}/(\gamma_{\rm diss}+\gamma_{\rm pump})$, and γ and Γ are defined by Eqs. (9) and (10). Equation (23) reproduces the results obtained in Ref. [85]. A wide filter allows almost all the light from the TLS and does not distort its statistics. Thus, the drop in $g_F^{(2)}(T,0)$ is expected for wide filters.

Figure 3 shows the dependence of $g_F^{(2)}(T,0)$, at $T \ll 1/\gamma_{\rm diss}$, on the filter width and the longitudinal relaxation rate [Eq. (10)]. At large filter width $\gamma_F \gg \gamma_{\rm diss}+\gamma_{\rm deph}$, we obtain $g_F^{(2)}(T,0) \approx 0$, which corresponds to the absence of the spectral filter. However, at $T < \gamma_F^{-1}$, the second-order autocorrelation function is in the range from 1/5 to 2/3 depending on the ratio between the transverse relaxation time and the duration of the pump pulse (Fig. 3). The naive suggestion might be $g_F^{(2)}(T,0) \approx 0$ at $T \ll \gamma_{\rm diss}$, because for fixed $\gamma_{\rm pump}$ the lower T is, the less the probability of two consequent acts of TLS excitation and light emission. However, Fig. 3 shows

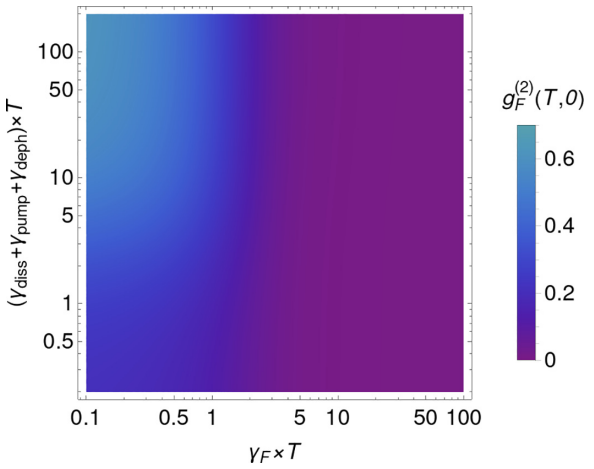

FIG. 3. The dependence of $g_F^{(2)}(T,0)$ on the filter width and the transverse relaxation rate in the limit of $T\gamma_{\rm diss} \ll 1$.

that $g_F^{(2)}(T,0)$ strongly differs from zero in this limit. We attribute this behavior to the correlations in the light emitted by the TLS. The second-order coherence function corresponding to the incoherent pump is 2, which means that the

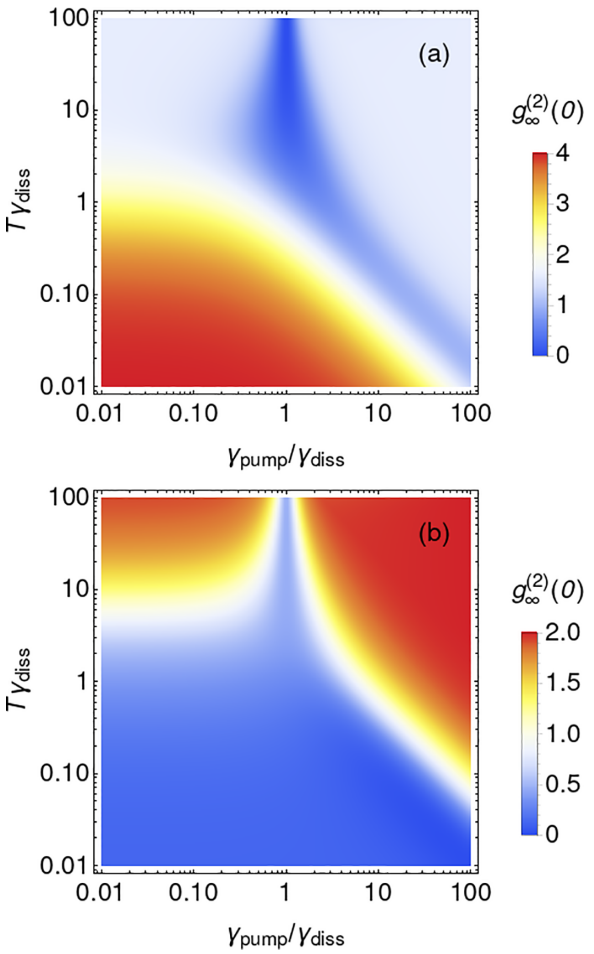

FIG. 4. The dependence of $g_\infty^{(2)}(0)$ on the pumping speed $\gamma_{\rm pump}$ and the duration of the pump pulse, T, at (a) $\gamma_{\rm deph} = 0$ and (b) $\gamma_{\rm deph} = 10\gamma_{\rm diss}$.

dispersion of the incoherent pump is significantly above the quantum limit. We suggest that the TLS translates this dispersion to the strong correlations of the emitted light at different moments in time, which results in the nonzero $g_F^{(2)}(T,0)$ in the limit of narrow filters and short pulse duration of the pump. Physically, nonzero $g_F^{(2)}(T,0)$ means that during the time γ_F^{-1}, the TLS has a nonzero probability of emitting two consequent photons. This process may happen even when $T \ll \gamma_{\text{diss}}$.

B. Long detector response time: Field integration

In the case $\tau \gg \tau_{\text{TLS}}$, we have $\hat{E}_{D,F}(t) \approx \int_0^{+\infty} \hat{E}_F(t+\tau)d\tau$. One can show that (see Appendix B)

$$\int_0^{+\infty} \hat{E}_F(\tau)d\tau = A\int_0^{+\infty} \hat{E}(\tau)d\tau, \tag{24}$$

where $A = \int_0^{+\infty} dt\, f(t) = \text{const}$. Therefore, in the case $\tau \gg \tau_{\text{TLS}}$, the second-order autocorrelation function is not dependent on the spectral filter

$$g_{\infty}^{(2)}(0) = \frac{\langle \int_0^{\infty} \hat{E}^{\dagger}(t_1)dt_1 \int_0^{\infty} \hat{E}^{\dagger}(t_2)dt_2 \int_0^{\infty} \hat{E}(t_3)dt_3 \int_0^{\infty} \hat{E}(t_4)dt_4\rangle}{\langle \int_0^{\infty} \hat{E}^{\dagger}(t_1)dt_1 \int_0^{\infty} \hat{E}(t_2)dt_2\rangle^2}, \tag{25}$$

where we assumed that the detector starts operating at $t = 0$. In this model of long detector response time, the detector integrates the electric field of the incoming light.

We express $g_{\infty}^{(2)}(0)$ in terms of operators $\hat{\sigma}$ and $\hat{\sigma}^{\dagger}$ in Appendix A. To evaluate Eq. (25), it is necessary to calculate the correlations $\langle \hat{\sigma}^{\dagger}(t_1)\hat{\sigma}(t_2)\rangle$ and $\langle \hat{\sigma}^{\dagger}(t_1)\hat{\sigma}^{\dagger}(t_2)\hat{\sigma}(t_3)\hat{\sigma}(t_4)\rangle$ for all possible time ratios $\{t_1, t_2, t_3, t_4\}$. Details of calculating these correlators using the generalized quantum regression theorem are in Appendix C.

Figure 4 shows that a good single-photon property is achievable at a short pump-pulse duration, $T \ll 1/\gamma_{\text{diss}}$, and a moderate pumping rate, $T\gamma_{\text{pump}} \lesssim 1$. In this case, we obtain

$$g_{\infty}^{(2)}(0) \approx \frac{4\gamma_{\text{diss}}}{\gamma_{\text{diss}} + \gamma_{\text{deph}}}. \tag{26}$$

Thus, at $T \ll 1/\gamma_{\text{diss}}$, $T\gamma_{\text{pump}} \lesssim 1$, and $\tau \gg \tau_{\text{TLS}}$, the second-order autocorrelation function decreases with increasing dephasing. This tendency is because the light emitted by the SPS with incoherent pumping has strong correlations [85]. An increase in dephasing leads to the destruction of these correlations, and as a result, $g_{\infty}^{(2)}(0)$ decreases (see Fig. 4).

C. Long detector response time: Intensity integration

If τ is the duration of the interaction between light and electrons and $\tau \gg \tau_{\text{TLS}}$, one can notice that the second-order autocorrelation function is equal to [73]

$$g_{\infty,F}^{(2)}(0) = \frac{\int_0^{\infty} dt_1 \int_0^{\infty} dt_2 \langle \mathcal{T}_{\rightarrow}\{\hat{E}_F^{\dagger}(t_1)\hat{E}_F^{\dagger}(t_2)\}\mathcal{T}_{\leftarrow}\{\hat{E}_F(t_2)\hat{E}_F(t_1)\}\rangle}{\left(\int_0^{\infty} dt \langle \hat{E}_F^{\dagger}(t)\hat{E}_F(t)\rangle\right)^2}. \tag{27}$$

In this model of long detector response time, the detector integrates the intensity of the incoming light. The example of such a detector is the EMCCD camera, where the typical exposure time is of the order of milliseconds [82,83].

We express $g_{\infty,F}^{(2)}(0)$ in terms of operators $\hat{\sigma}$ and $\hat{\sigma}^{\dagger}$ in Appendix A. To evaluate Eq. (27), it is necessary to calculate the correlations $\langle \hat{\sigma}^{\dagger}(t_1)\hat{\sigma}(t_2)\rangle$ and $\langle \hat{\sigma}^{\dagger}(t_1)\hat{\sigma}^{\dagger}(t_2)\hat{\sigma}(t_3)\hat{\sigma}(t_4)\rangle$ for all possible time orderings $\{t_1, t_2, t_3, t_4\}$. Details of calculating of these correlators using the generalized quantum regression theorem are given in Appendix C.

In the absence of a spectral filter, we obtain the following second-order autocorrelation function

$$g_{\infty,F}^{(2)}(0)|_{\text{no filter}} = -\frac{2(1-3p-pT\gamma)(1-p)e^{T\gamma}}{\{p-e^{T\gamma}[p+(1-p)T\gamma]\}^2} + \frac{[2(1-3p)-2T\gamma(1-2p)+(T\gamma)^2(1-p)](1-p)e^{2T\gamma}}{\{p-e^{T\gamma}[p+(1-p)T\gamma]\}^2}, \tag{28}$$

which monotonously rises from 0 to 1 as the pump-pulse duration increases.

Figure 5 shows that a good single-photon property is achievable at $T \lesssim 1/\gamma_{\text{diss}}$ and does not depend on the filter width in this case. The case $\gamma_F \gg \gamma_{\text{diss}}$ corresponds to the absence of the spectral filter, and thus $g_{\infty,F}^{(2)}(0) \approx g_{\infty,F}^{(2)}(0)|_{\text{no filter}}$. At $\gamma_F \ll \gamma_{\text{diss}}$ and $T \gg 1/\gamma_{\text{diss}}$, we see the parameter region where $g_{\infty,F}^{(2)}(0)$ demonstrates strong bunching.

Interestingly, $g_F^{(2)}(T,0)$ and $g_{\infty,F}^{(2)}(0)$ behave differently as the filter width narrows. For $g_F^{(2)}(T,0)$ at narrow filter widths, one cannot fully compensate the increase in the second-order correlation function by decreasing the pulse duration time (Fig. 2). However, one can achieve such compensation for $g_{\infty,F}^{(2)}(0)$ (Fig. 5). This also means that the second-order autocorrelation function measured with the detector with long exposure time can be lower than the actual second-order autocorrelation function.

V. QUANTUM YIELD

Due to frequency filtering, not all the light from the TLS can reach the detector, which lowers the quantum yield of the SPS. We denote the quantum yield in the absence of a spectral filter as QY, and in the presence of the spectral filter as QY_F. The ratio between QY_F and QY can be calculated according to [76]

$$\frac{\text{QY}_F}{\text{QY}} = \frac{\int_{-\infty}^{+\infty} dt \langle \hat{E}_F^{\dagger}(t)\hat{E}_F(t)\rangle}{\int_{-\infty}^{+\infty} dt \langle \hat{E}^{\dagger}(t)\hat{E}(t)\rangle}. \tag{29}$$

We present QY_F/QY in terms of operators $\hat{\sigma}$ and $\hat{\sigma}^{\dagger}$ in Appendix A. To obtain QY_F/QY, it is necessary to calculate $\langle \hat{\sigma}^{\dagger}(t_1)\hat{\sigma}(t_2)\rangle$. This calculation requires the quantum regression theorem [49,74].

At short pump-pulse duration, $T \ll \gamma_{\text{diss}}^{-1}$, the decrease in quantum yield does not depend on the γ_{pump}:

$$\frac{\text{QY}_F}{\text{QY}} \approx \frac{2\gamma_F}{\gamma_{\text{diss}} + \gamma_{\text{deph}} + 2\gamma_F}. \tag{30}$$

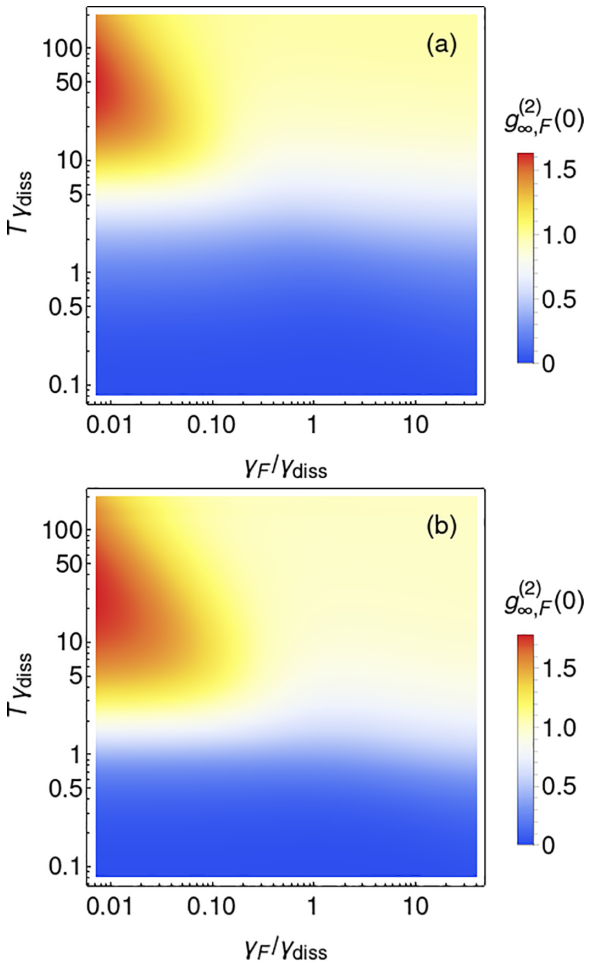

FIG. 5. The dependence of $g^{(2)}_{\infty,F}(0)$ on the filter width γ_F and the pump-pulse duration T at $\gamma_{\rm deph} = 10\gamma_{\rm diss}$ in the case of (a) $\gamma_{\rm pump} = 0.01\gamma_{\rm diss}$ and (b) $\gamma_{\rm pump} = 5\gamma_{\rm diss}$.

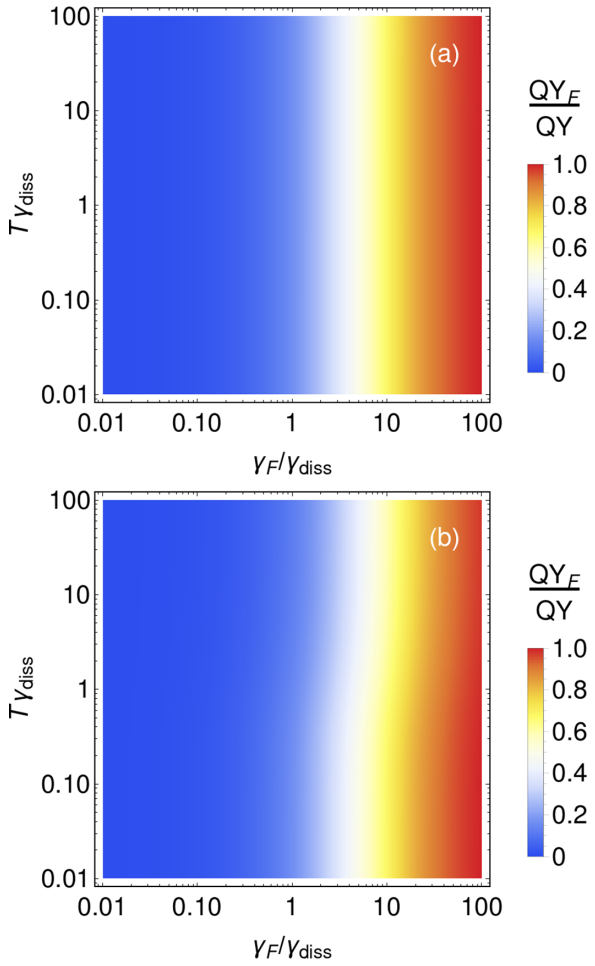

FIG. 6. The dependence of the quantum yield on the filter width γ_F and the pump-pulse duration T at $\gamma_{\rm deph} = 10\gamma_{\rm diss}$ in the case (a) $\gamma_{\rm pump} = 0.01\gamma_{\rm diss}$ and (b) $\gamma_{\rm pump} = 5\gamma_{\rm diss}$.

When the duration of the pump pulse is long enough, $T \gg \gamma_{\rm diss}^{-1}$, we obtain the approximate expression for the decrease in quantum yield:

$$\frac{\rm QY_F}{\rm QY} \approx \frac{2\gamma_F}{\gamma_{\rm diss} + \gamma_{\rm deph} + \gamma_{\rm pump} + 2\gamma_F}. \tag{31}$$

Figure 6 shows the dependence of the quantum yield on the spectral filter width and the duration of the pump pulse. In the presence of the spectral filter, the quantum yield of the SPS drops from 1 to 0 when the filter width decreases. The sharp decrease in $\rm QY_F/QY$ occurs at $\gamma_F \sim \gamma_{\rm diss}$. From Eq. (10), it follows that the transverse relaxation rate of the TLS grows as the pumping rate increases. This trend leads to an increase in the spectral width of the light emitted by the TLS. Therefore, when the pump pulse is long enough, an increase in the rate of incoherent pumping with a fixed spectral filter leads to a decrease in quantum efficiency.

VI. CONCLUSION

In this paper, we investigated the possibility of using a spectral filter to control the purity, the indistinguishability, and the quantum yield of the light emitted by SPSs. We showed that it is possible to achieve near-unity indistinguishability even at fast dephasing rates by applying the spectral filter with a small width, $\gamma_F \ll \gamma_{\rm diss}$, and a short pump-pulse duration, $T \ll 1/\gamma_{\rm diss}$. In this case, the second-order autocorrelation function lies between 1/5 and 2/3 depending on the ratio between the transverse relaxation time and the pump duration. The single-photon properties of the light manifest themselves differently, depending on the response time of the quantum system, on which the light from the SPS acts. In particular, the second-order autocorrelation function of the light measured with a detector with long exposure time, e.g., an EMCCD camera, can be lower than the actual autocorrelation function of the light emitted by the SPS and passed through the spectral filter. A compromise of high indistinguishability and high photon purity with the effective quantum yield is difficult to achieve because narrowing the width of the spectral filter reduces the intensity of the light passing through the filter. Thus, the significant improvement in the indistinguishability and the purity of the SPS by applying a spectral filter is possible only by significantly reducing the quantum yield of this SPS.

In the framework of our model, the filter does not affect the dynamics of the SPS in any way, but only transforms its radiation. Therefore, our theory is directly applicable, only if the filter is included in the optical path between the SPS and the detector. Such a situation is realized in photonic integrated circuits with add-drop filters [86,87]. We emphasize that not all implementations of frequency filtering can be covered by the present theory. For example, placing an SPS near a plasmonic nanoantenna results in frequency filtering, but also affects the dynamics of an SPS due to the Purcell factor [88–90]. The applicability of the developed theory to the case when the SPS and the filter are combined via interface and the filter changes dynamics of the SPS is beyond the scope of this article.

ACKNOWLEDGMENTS

The research was financially supported by a grant from the Russian Science Foundation (Project No. 20-72-10057). V.Yu.S. thanks the Foundation for the Advancement of Theoretical Physics and Mathematics "Basis."

APPENDIX A: EXPRESSIONS FOR I_F, $g_F^{(2)}(T,0)$, $g_\infty^{(2)}(0)$, AND $\mathrm{QY}_F/\mathrm{QY}$ THROUGH $\hat{\sigma}$

To express I_F, $g_F^{(2)}(T,0)$, $g_\infty^{(2)}(0)$, $g_{\infty,F}^{(2)}(0)$, and $\mathrm{QY}_F/\mathrm{QY}$ in terms of TLS operators, we use Eq. (14) and the connection between $\hat{E}(t)$ and $\hat{\sigma}(t)$ given by Eq. (11). In the expressions below, we also assume that until the moment $t=0$ the TLS is in the ground state. From Eq. (16), we obtain

$$I_F = \frac{\int_0^{+\infty} dt_1 \int_0^{+\infty} dt_2 \int_0^{+\infty} dt_3 \int_0^{+\infty} dt_4 x(t_1-t_3) x^*(t_2-t_4) \langle \hat{\sigma}^\dagger(t_1)\hat{\sigma}(t_2)\rangle \langle \hat{\sigma}^\dagger(t_3)\hat{\sigma}(t_4)\rangle^*}{\left(\int_0^{+\infty} dt_1 \int_0^{+\infty} x(t_1-t_2)\langle \hat{\sigma}^\dagger(t_1)\hat{\sigma}(t_2)\rangle\right)^2}, \tag{A1}$$

where we introduce the notation

$$x(\Delta t) = \int_{-\infty}^{+\infty} \frac{d\omega}{2\pi} |F(\omega)|^2 e^{-i\omega\Delta t}. \tag{A2}$$

From Eq. (21), Eq. (25), and Eq. (27), we obtain

$$g_F^{(2)}(t,0) = \frac{\int_0^t dt_1 \int_0^t dt_2 \int_0^t dt_3 \int_0^t dt_4 f^*(t-t_1) f^*(t-t_2) f(t-t_3) f(t-t_4) \langle \hat{\sigma}^\dagger(t_1)\hat{\sigma}^\dagger(t_2)\hat{\sigma}(t_3)\hat{\sigma}(t_4)\rangle}{\left(\int_0^t dt_1 \int_0^t dt_2 f^*(t-t_1) f(t-t_2)\langle \hat{\sigma}^\dagger(t_1)\hat{\sigma}(t_2)\rangle\right)^2}, \tag{A3}$$

$$g_\infty^{(2)}(0) = \frac{\int_0^{+\infty} dt_1 \int_0^{+\infty} dt_2 \int_0^{+\infty} dt_3 \int_0^{+\infty} dt_4 \langle \hat{\sigma}^\dagger(t_1)\hat{\sigma}^\dagger(t_2)\hat{\sigma}(t_3)\hat{\sigma}(t_4)\rangle}{\left(\int_0^{+\infty} dt_1 \int_0^{+\infty} dt_2 \langle \hat{\sigma}^\dagger(t_1)\hat{\sigma}(t_2)\rangle\right)^2}, \tag{A4}$$

$$g_{\infty,F}^{(2)}(0) = \frac{2\int_0^{+\infty} dt_2 \int_0^{t_2} dt_1 \int_0^{t_1} dt_1' \int_0^{t_2} dt_2' \int_0^{t_2} dt_3' \int_0^{t_1} dt_4' f^*(t_1-t_1') f^*(t_2-t_2') f(t_2-t_3') f(t_1-t_4') \langle \hat{\sigma}^\dagger(t_1')\hat{\sigma}^\dagger(t_2')\hat{\sigma}(t_3')\hat{\sigma}(t_4')\rangle}{\left(\int_0^{+\infty} dt \int_0^t dt_1 \int_0^t dt_2 f^*(t-t_1) f(t-t_2)\langle \hat{\sigma}^\dagger(t_1)\hat{\sigma}(t_2)\rangle\right)^2}. \tag{A5}$$

From Eq. (14), we obtain

$$\frac{\mathrm{QY}_F}{\mathrm{QY}} = \frac{\int_0^{+\infty} dt \int_0^t dt_1 \int_0^t dt_2 f^*(t-t_1) f(t-t_2)\langle \hat{\sigma}^\dagger(t_1)\hat{\sigma}(t_2)\rangle}{\int_0^{+\infty} dt \langle \hat{\sigma}^\dagger(t)\hat{\sigma}(t)\rangle}. \tag{A6}$$

APPENDIX B: PROOF OF EQ. (24)

To prove Eq. (24), we use Eq. (14) and the initial conditions described in Sec. II:

$$\int_0^{+\infty} \hat{E}_F(t)dt = \int_0^{+\infty} dt \int_0^t dt' f(t-t')\hat{E}(t') = \int_0^{+\infty} dt' \hat{E}(t') \int_{t'}^{+\infty} dt f(t-t') = \int_0^{+\infty} f(t)dt \int_0^{+\infty} \hat{E}(t')dt'. \tag{B1}$$

APPENDIX C: CALCULATION OF $\langle \hat{\sigma}^\dagger(t_1)\hat{\sigma}^\dagger(t_2)\hat{\sigma}(t_3)\hat{\sigma}(t_4)\rangle$

The correlator $\langle \hat{\sigma}^\dagger(t_1)\hat{\sigma}^\dagger(t_2)\hat{\sigma}(t_3)\hat{\sigma}(t_4)\rangle$ with an arbitrary ratio of times can be calculated analytically using a generalized quantum regression theorem [84]. For t_1, t_2, t_3, $t_4 \leqslant T$, the exact expression for the correlation $\langle \hat{\sigma}^\dagger(t_1)\hat{\sigma}^\dagger(t_2)\hat{\sigma}(t_3)\hat{\sigma}(t_4)\rangle$ is given in the Supporting Information to the article [85]. For the remaining time relations t_1, t_2, t_3, t_4, and T, explicit expressions for $\langle \hat{\sigma}^\dagger(t_1)\hat{\sigma}^\dagger(t_2)\hat{\sigma}(t_3)\hat{\sigma}(t_4)\rangle$ are given below:

$$\langle \hat{\sigma}^\dagger(t_1)\hat{\sigma}^\dagger(t_2)\hat{\sigma}(t_3)\hat{\sigma}(t_4)\rangle = \langle \hat{\sigma}^\dagger(t_1)\hat{\sigma}^\dagger(t_2)\hat{\sigma}(t_3)\hat{\sigma}(T)\rangle e^{-(\gamma_{\mathrm{diss}}+\gamma_{\mathrm{deph}}+2i\omega_0)(t_4-T)/2}, \quad t_1,\, t_2,\, t_3 \leqslant T, \quad t_4 > T, \tag{C1}$$

$$\langle \hat{\sigma}^\dagger(t_1)\hat{\sigma}^\dagger(t_2)\hat{\sigma}(t_3)\hat{\sigma}(t_4)\rangle = \langle \hat{\sigma}^\dagger(t_1)\hat{\sigma}^\dagger(t_2)\hat{\sigma}(T)\hat{\sigma}(t_4)\rangle e^{-(\gamma_{\mathrm{diss}}+\gamma_{\mathrm{deph}}+2i\omega_0)(t_3-T)/2}, \quad t_1,\, t_2,\, t_4 \leqslant T, \quad t_3 > T, \tag{C2}$$

$$\langle \hat{\sigma}^\dagger(t_1)\hat{\sigma}^\dagger(t_2)\hat{\sigma}(t_3)\hat{\sigma}(t_4)\rangle = \langle \hat{\sigma}^\dagger(t_1)\hat{\sigma}^\dagger(T)\hat{\sigma}(t_3)\hat{\sigma}(t_4)\rangle e^{-(\gamma_{\mathrm{diss}}+\gamma_{\mathrm{deph}}-2i\omega_0)(t_2-T)/2}, \quad t_1,\, t_3,\, t_4 \leqslant T, \quad t_2 > T, \tag{C3}$$

$$\langle\hat{\sigma}^\dagger(t_1)\hat{\sigma}^\dagger(t_2)\hat{\sigma}(t_3)\hat{\sigma}(t_4)\rangle = \langle\hat{\sigma}^\dagger(T)\hat{\sigma}^\dagger(t_2)\hat{\sigma}(t_3)\hat{\sigma}(t_4)\rangle e^{-(\gamma_{\rm diss}+\gamma_{\rm deph}-2i\omega_0)(t_1-T)/2}, \quad t_2,\, t_3,\, t_4 \leqslant T, \quad t_1 > T, \tag{C4}$$

$$\langle\hat{\sigma}^\dagger(t_1)\hat{\sigma}^\dagger(t_2)\hat{\sigma}(t_3)\hat{\sigma}(t_4)\rangle = \langle\hat{\sigma}^\dagger(t_1)\hat{\sigma}^\dagger(T)\hat{\sigma}(t_3)\hat{\sigma}(T)\rangle e^{-(\gamma_{\rm diss}+\gamma_{\rm deph})|t_2-t_4|/2} e^{-i\omega_0(t_4-t_2)} e^{-\gamma_{\rm diss}(\min\{t_2,t_4\}-T)}, \quad t_1,\, t_3 \leqslant T, \quad t_2,\, t_4 > T, \tag{C5}$$

$$\langle\hat{\sigma}^\dagger(t_1)\hat{\sigma}^\dagger(t_2)\hat{\sigma}(t_3)\hat{\sigma}(t_4)\rangle = \langle\hat{\sigma}^\dagger(T)\hat{\sigma}^\dagger(t_2)\hat{\sigma}(t_3)\hat{\sigma}(T)\rangle e^{-(\gamma_{\rm diss}+\gamma_{\rm deph})|t_1-t_4|/2} e^{-i\omega_0(t_4-t_1)} e^{-\gamma_{\rm diss}(\min\{t_1,t_4\}-T)}, \quad t_2,\, t_3 \leqslant T, \quad t_1,\, t_4 > T, \tag{C6}$$

$$\langle\hat{\sigma}^\dagger(t_1)\hat{\sigma}^\dagger(t_2)\hat{\sigma}(t_3)\hat{\sigma}(t_4)\rangle = \langle\hat{\sigma}^\dagger(T)\hat{\sigma}^\dagger(t_2)\hat{\sigma}(T)\hat{\sigma}(t_4)\rangle e^{-(\gamma_{\rm diss}+\gamma_{\rm deph})|t_1-t_3|/2} e^{-i\omega_0(t_3-t_1)} e^{-\gamma_{\rm diss}(\min\{t_1,t_3\}-T)}, \quad t_2,\, t_4 \leqslant T, \quad t_1,\, t_3 > T, \tag{C7}$$

$$\langle\hat{\sigma}^\dagger(t_1)\hat{\sigma}^\dagger(t_2)\hat{\sigma}(t_3)\hat{\sigma}(t_4)\rangle = \langle\hat{\sigma}^\dagger(t_1)\hat{\sigma}^\dagger(T)\hat{\sigma}(T)\hat{\sigma}(t_4)\rangle e^{-(\gamma_{\rm diss}+\gamma_{\rm deph})|t_2-t_3|/2} e^{-i\omega_0(t_3-t_2)} e^{-\gamma_{\rm diss}(\min\{t_2,t_3\}-T)}, \quad t_1,\, t_4 \leqslant T, \quad t_2,\, t_3 > T, \tag{C8}$$

$$\langle\hat{\sigma}^\dagger(t_1)\hat{\sigma}^\dagger(t_2)\hat{\sigma}(t_3)\hat{\sigma}(t_4)\rangle = 0, \quad t_1,\, t_2 \leqslant T, \quad t_3,\, t_4 > T, \tag{C9}$$

$$\langle\hat{\sigma}^\dagger(t_1)\hat{\sigma}^\dagger(t_2)\hat{\sigma}(t_3)\hat{\sigma}(t_4)\rangle = 0, \quad t_3,\, t_4 \leqslant T, \quad t_1,\, t_2 > T, \tag{C10}$$

$$\langle\hat{\sigma}^\dagger(t_1)\hat{\sigma}^\dagger(t_2)\hat{\sigma}(t_3)\hat{\sigma}(t_4)\rangle = 0, \quad t_4 \leqslant T, \quad t_1,\, t_2,\, t_3 > T, \tag{C11}$$

$$\langle\hat{\sigma}^\dagger(t_1)\hat{\sigma}^\dagger(t_2)\hat{\sigma}(t_3)\hat{\sigma}(t_4)\rangle = 0, \quad t_3 \leqslant T, \quad t_1,\, t_2,\, t_4 > T, \tag{C12}$$

$$\langle\hat{\sigma}^\dagger(t_1)\hat{\sigma}^\dagger(t_2)\hat{\sigma}(t_3)\hat{\sigma}(t_4)\rangle = 0, \quad t_2 \leqslant T, \quad t_1,\, t_3,\, t_4 > T, \tag{C13}$$

$$\langle\hat{\sigma}^\dagger(t_1)\hat{\sigma}^\dagger(t_2)\hat{\sigma}(t_3)\hat{\sigma}(t_4)\rangle = 0, \quad t_1 \leqslant T, \quad t_2,\, t_3,\, t_4 > T, \tag{C14}$$

$$\langle\hat{\sigma}^\dagger(t_1)\hat{\sigma}^\dagger(t_2)\hat{\sigma}(t_3)\hat{\sigma}(t_4)\rangle = 0, \quad t_1,\, t_2,\, t_3,\, t_4 > T. \tag{C15}$$

[1] R. J. Hughes, D. M. Alde, P. Dyer, G. G. Luther, G. L. Morgan, and M. Schauer, Quantum cryptography, Contemp. Phys. **36**, 149 (1995).

[2] A. Beveratos, R. Brouri, T. Gacoin, A. Villing, J.-P. Poizat, and P. Grangier, Single Photon Quantum Cryptography, Phys. Rev. Lett. **89**, 187901 (2002).

[3] B. Lounis and M. Orrit, Single-photon sources, Rep. Prog. Phys. **68**, 1129 (2005).

[4] M. Gschrey, A. Thoma, P. Schnauber, M. Seifried, R. Schmidt, B. Wohlfeil, L. Krüger, J.-H. Schulze, T. Heindel, S. Burger *et al.*, Highly indistinguishable photons from deterministic quantum-dot microlenses utilizing three-dimensional *in situ* electron-beam lithography, Nat. Commun. **6**, 7662 (2015).

[5] O. Gazzano, S. Michaelis de Vasconcellos, C. Arnold, A. Nowak, E. Galopin, I. Sagnes, L. Lanco, A. Lemaître, and P. Senellart, Bright solid-state sources of indistinguishable single photons, Nat. Commun. **4**, 1425 (2013).

[6] J. L. O'Brien, Optical quantum computing, Science **318**, 1567 (2007).

[7] X.-D. Cai, C. Weedbrook, Z.-E. Su, M.-C. Chen, M. Gu, M.-J. Zhu, L. Li, N.-L. Liu, C.-Y. Lu, and J.-W. Pan, Experimental Quantum Computing to Solve Systems of Linear Equations, Phys. Rev. Lett. **110**, 230501 (2013).

[8] P. Michler, *Quantum Dots for Quantum Information Technologies*, Nano-optics and Nanophotonics Vol. 237 (Springer, Berlin, 2017).

[9] B. P. Lanyon, J. D. Whitfield, G. G. Gillett, M. E. Goggin, M. P. Almeida, I. Kassal, J. D. Biamonte, M. Mohseni, B. J. Powell, M. Barbieri *et al.*, Towards quantum chemistry on a quantum computer, Nat. Chem. **2**, 106 (2010).

[10] M. von Helversen, J. Böhm, M. Schmidt, M. Gschrey, J.-H. Schulze, A. Strittmatter, S. Rodt, J. Beyer, T. Heindel, and S. Reitzenstein, Quantum metrology of solid-state single-photon sources using photon-number-resolving detectors, New J. Phys. **21**, 035007 (2019).

[11] K. R. Motes, R. L. Mann, J. P. Olson, N. M. Studer, E. A. Bergeron, A. Gilchrist, J. P. Dowling, D. W. Berry, and P. P. Rohde, Efficient recycling strategies for preparing large Fock states from single-photon sources: Applications to quantum metrology, Phys. Rev. A **94**, 012344 (2016).

[12] M. Förtsch, J. U. Fürst, C. Wittmann, D. Strekalov, A. Aiello, M. V. Chekhova, C. Silberhorn, G. Leuchs, and C. Marquardt, A versatile source of single photons for quantum information processing, Nat. Commun. **4**, 1818 (2013).

[13] T. M. Babinec, B. J. Hausmann, M. Khan, Y. Zhang, J. R. Maze, P. R. Hemmer, and M. Lončar, A diamond nanowire single-photon source, Nat. Nanotechnol. **5**, 195 (2010).

[14] A. W. Elshaari, I. E. Zadeh, A. Fognini, M. E. Reimer, D. Dalacu, P. J. Poole, V. Zwiller, and K. D. Jöns, On-chip single photon filtering and multiplexing in hybrid quantum photonic circuits, Nat. Commun. **8**, 379 (2017).

[15] A. Singh, Q. Li, S. Liu, Y. Yu, X. Lu, C. Schneider, S. Höfling, J. Lawall, V. Verma, R. Mirin *et al.*, Quantum frequency conversion of a quantum dot single-photon source on a nanophotonic chip, Optica **6**, 563 (2019).

[16] F. Bouchard, A. Sit, Y. Zhang, R. Fickler, F. M. Miatto, Y. Yao, F. Sciarrino, and E. Karimi, Two-photon interference: The Hong–Ou–Mandel effect, Rep. Prog. Phys. **84**, 012402 (2021).

[17] C. Lang, C. Eichler, L. Steffen, J. Fink, M. J. Woolley, A. Blais, and A. Wallraff, Correlations, indistinguishability and entanglement in Hong–Ou–Mandel experiments at microwave frequencies, Nat. Phys. **9**, 345 (2013).

[18] R. Lopes, A. Imanaliev, A. Aspect, M. Cheneau, D. Boiron, and C. I. Westbrook, Atomic Hong–Ou–Mandel experiment, Nature (London) **520**, 66 (2015).

[19] R. J. Lewis-Swan, Proposal for demonstrating the Hong–Ou–Mandel effect with matter waves, in *Ultracold Atoms for Foundational Tests of Quantum Mechanics* (Springer, Berlin, 2016), pp. 45–55.

[20] A. Saxena, Y. Chen, A. Ryou, C. G. Sevilla, P. Xu, and A. Majumdar, Improving indistinguishability of single photons from colloidal quantum dots using nanocavities, ACS Photonics **6**, 3166 (2019).

[21] P. Borri, W. Langbein, S. Schneider, U. Woggon, R. L. Sellin, D. Ouyang, and D. Bimberg, Ultralong Dephasing Time in InGaAs Quantum Dots, Phys. Rev. Lett. **87**, 157401 (2001).

[22] S. Kako, C. Santori, K. Hoshino, S. Götzinger, Y. Yamamoto, and Y. Arakawa, A gallium nitride single-photon source operating at 200 K, Nat. Mater. **5**, 887 (2006).

[23] J. Bylander, I. Robert-Philip, and I. Abram, Interference and correlation of two independent photons, Eur. Phys. J. D **22**, 295 (2003).

[24] T. Grange, G. Hornecker, D. Hunger, J.-P. Poizat, J.-M. Gérard, P. Senellart, and A. Auffèves, Cavity-Funneled Generation of Indistinguishable Single Photons from Strongly Dissipative Quantum Emitters, Phys. Rev. Lett. **114**, 193601 (2015).

[25] P. Borri, W. Langbein, U. Woggon, V. Stavarache, D. Reuter, and A. D. Wieck, Exciton dephasing via phonon interactions in inas quantum dots: Dependence on quantum confinement, Phys. Rev. B **71**, 115328 (2005).

[26] A. Thoma, P. Schnauber, M. Gschrey, M. Seifried, J. Wolters, J.-H. Schulze, A. Strittmatter, S. Rodt, A. Carmele, A. Knorr *et al.*, Exploring Dephasing of a Solid-State Quantum Emitter via Time- and Temperature-Dependent Hong-Ou-Mandel Experiments, Phys. Rev. Lett. **116**, 033601 (2016).

[27] H. Choi, D. Zhu, Y. Yoon, and D. Englund, Cascaded Cavities Boost the Indistinguishability of Imperfect Quantum Emitters, Phys. Rev. Lett. **122**, 183602 (2019).

[28] D. Englund, D. Fattal, E. Waks, G. Solomon, B. Zhang, T. Nakaoka, Y. Arakawa, Y. Yamamoto, and J. Vučković, Controlling the Spontaneous Emission Rate of Single Quantum Dots in a Two-Dimensional Photonic Crystal, Phys. Rev. Lett. **95**, 013904 (2005).

[29] C. P. Dietrich, A. Fiore, M. G. Thompson, M. Kamp, and S. Höfling, Gaas integrated quantum photonics: Towards compact and multi-functional quantum photonic integrated circuits, Laser Photonics Rev. **10**, 870 (2016).

[30] A. Kiraz, M. Atatüre, and A. Imamoğlu, Quantum-dot single-photon sources: Prospects for applications in linear optics quantum-information processing, Phys. Rev. A **69**, 032305 (2004).

[31] K. Hennessy, A. Badolato, M. Winger, D. Gerace, M. Atatüre, S. Gulde, S. Fält, E. L. Hu, and A. Imamoğlu, Quantum nature of a strongly coupled single quantum dot–cavity system, Nature (London) **445**, 896 (2007).

[32] P. Kaer, P. Lodahl, A.-P. Jauho, and J. Mork, Microscopic theory of indistinguishable single-photon emission from a quantum dot coupled to a cavity: The role of non-Markovian phonon-induced decoherence, Phys. Rev. B **87**, 081308(R) (2013).

[33] F. Liu, A. J. Brash, J. O'Hara, L. M. Martins, C. L. Phillips, R. J. Coles, B. Royall, E. Clarke, C. Bentham, N. Prtljaga *et al.*, High purcell factor generation of indistinguishable on-chip single photons, Nat. Nanotechnol. **13**, 835 (2018).

[34] F. W. Sun and C. W. Wong, Indistinguishability of independent single photons, Phys. Rev. A **79**, 013824 (2009).

[35] H. Mäntynen, N. Anttu, Z. Sun, and H. Lipsanen, Single-photon sources with quantum dots in III–V nanowires, Nanophotonics **8**, 747 (2019).

[36] A. Laucht, N. Hauke, J. M. Villas-Bôas, F. Hofbauer, G. Böhm, M. Kaniber, and J. J. Finley, Dephasing of Exciton Polaritons in Photoexcited InGaAs Quantum Dots in GaAs Nanocavities, Phys. Rev. Lett. **103**, 087405 (2009).

[37] P. Senellart, G. Solomon, and A. White, High-performance semiconductor quantum-dot single-photon sources, Nat. Nanotechnol. **12**, 1026 (2017).

[38] S. Hughes and H. Carmichael, Phonon-mediated population inversion in a semiconductor quantum-dot cavity system, New J. Phys. **15**, 053039 (2013).

[39] J. H. Quilter, A. J. Brash, F. Liu, M. Glässl, A. M. Barth, V. M. Axt, A. J. Ramsay, M. S. Skolnick, and A. M. Fox, Phonon-Assisted Population Inversion of a Single InGaAs/GaAs Quantum Dot by Pulsed Laser Excitation, Phys. Rev. Lett. **114**, 137401 (2015).

[40] Z. Yuan, B. E. Kardynal, R. M. Stevenson, A. J. Shields, C. J. Lobo, K. Cooper, N. S. Beattie, D. A. Ritchie, and M. Pepper, Electrically driven single-photon source, Science **295**, 102 (2002).

[41] J. Zhang, J. S. Wildmann, F. Ding, R. Trotta, Y. Huo, E. Zallo, D. Huber, A. Rastelli, and O. G. Schmidt, High yield and ultrafast sources of electrically triggered entangled-photon pairs based on strain-tunable quantum dots, Nat. Commun. **6**, 10067 (2015).

[42] A. Poshakinskiy and A. Poddubny, Time-dependent photon correlations for incoherently pumped quantum dot strongly coupled to the cavity mode, J. Exp. Theor. Phys. **118**, 205 (2014).

[43] R. B. Patel, A. J. Bennett, K. Cooper, P. Atkinson, C. A. Nicoll, D. A. Ritchie, and A. J. Shields, Quantum interference of electrically generated single photons from a quantum dot, Nanotechnology **21**, 274011 (2010).

[44] J. Lee, E. Murray, A. Bennett, D. Ellis, C. Dangel, I. Farrer, P. Spencer, D. A. Ritchie, and A. Shields, Electrically driven and electrically tunable quantum light sources, Appl. Phys. Lett. **110**, 071102 (2017).

[45] Y. Arakawa and M. J. Holmes, Progress in quantum-dot single photon sources for quantum information technologies: A broad spectrum overview, Appl. Phys. Rev. **7**, 021309 (2020).

[46] A. Boretti, L. Rosa, A. Mackie, and S. Castelletto, Electrically driven quantum light sources, Adv. Opt. Mater. **3**, 1012 (2015).

[47] L. Zhang, Y.-J. Yu, L.-G. Chen, Y. Luo, B. Yang, F.-F. Kong, G. Chen, Y. Zhang, Q. Zhang, Y. Luo *et al.*, Electrically driven

single-photon emission from an isolated single molecule, Nat. Commun. **8**, 580 (2017).

[48] H. J. Carmichael, *Statistical Methods in Quantum Optics 1: Master Equations and Fokker-Planck Equations* (Springer, Berlin, 1999).

[49] H.-P. Breuer and F. Petruccione, *The Theory of Open Quantum Systems* (Oxford University, Oxford, 2002).

[50] S. Buckley, K. Rivoire, and J. Vučković, Engineered quantum dot single-photon sources, Rep. Prog. Phys. **75**, 126503 (2012).

[51] S. Strauf, N. G. Stoltz, M. T. Rakher, L. A. Coldren, P. M. Petroff, and D. Bouwmeester, High-frequency single-photon source with polarization control, Nat. Photon. **1**, 704 (2007).

[52] L. Hanschke, K. A. Fischer, S. Appel, D. Lukin, J. Wierzbowski, S. Sun, R. Trivedi, J. Vučković, J. J. Finley, and K. Müller, Quantum dot single-photon sources with ultra-low multi-photon probability, npj Quantum Inf. **4**, 43 (2018).

[53] P. Michler, A. Kiraz, C. Becher, W. Schoenfeld, P. Petroff, L. Zhang, E. Hu, and A. Imamoglu, A quantum dot single-photon turnstile device, Science **290**, 2282 (2000).

[54] D. Fattal, E. Diamanti, K. Inoue, and Y. Yamamoto, Quantum Teleportation with a Quantum Dot Single Photon Source, Phys. Rev. Lett. **92**, 037904 (2004).

[55] H. Ollivier, I. M. de Buy Wenniger, S. Thomas, S. C. Wein, A. Harouri, G. Coppola, P. Hilaire, C. Millet, A. Lemaitre, I. Sagnes *et al.*, Reproducibility of high-performance quantum dot single-photon sources, ACS Photonics **7**, 1050 (2020).

[56] M. Steiner, A. Hartschuh, R. Korlacki, and A. J. Meixner, Highly efficient, tunable single photon source based on single molecules, Appl. Phys. Lett. **90**, 183122 (2007).

[57] P. Lombardi, M. Trapuzzano, M. Colautti, G. Margheri, I. P. Degiovanni, M. López, S. Kück, and C. Toninelli, A molecule-based single-photon source applied in quantum radiometry, Adv. Quantum Technol. **3**, 1900083 (2020).

[58] I. Aharonovich, S. Castelletto, D. Simpson, C. Su, A. Greentree, and S. Prawer, Diamond-based single-photon emitters, Rep. Prog. Phys. **74**, 076501 (2011).

[59] R. Albrecht, A. Bommer, C. Deutsch, J. Reichel, and C. Becher, Coupling of a Single Nitrogen-Vacancy Center in Diamond to a Fiber-Based Microcavity, Phys. Rev. Lett. **110**, 243602 (2013).

[60] A. Faraon, C. Santori, Z. Huang, V. M. Acosta, and R. G. Beausoleil, Coupling of Nitrogen-Vacancy Centers to Photonic Crystal Cavities in Monocrystalline Diamond, Phys. Rev. Lett. **109**, 033604 (2012).

[61] E. Ampem-Lassen, D. Simpson, B. Gibson, S. Trpkovski, F. Hossain, S. Huntington, K. Ganesan, L. Hollenberg, and S. Prawer, Nano-manipulation of diamond-based single photon sources, Opt. Express **17**, 11287 (2009).

[62] J. Benedikter, H. Kaupp, T. Hümmer, Y. Liang, A. Bommer, C. Becher, A. Krueger, J. M. Smith, T. W. Hänsch, and D. Hunger, Cavity-Enhanced Single-Photon Source Based on the Silicon-Vacancy Center in Diamond, Phys. Rev. Appl. **7**, 024031 (2017).

[63] M. Toth and I. Aharonovich, Single photon sources in atomically thin materials, Annu. Rev. Phys. Chem. **70**, 123 (2019).

[64] A. Reserbat-Plantey, I. Epstein, I. Torre, A. T. Costa, P. Gonçalves, N. A. Mortensen, M. Polini, J. C. Song, N. M. Peres, and F. H. Koppens, Quantum nanophotonics in two-dimensional materials, ACS Photonics **8**, 85 (2021).

[65] V. Klimov, A. Mikhailovsky, S. Xu, A. Malko, J. Hollingsworth, C. Leatherdale, H.-J. Eisler, and M. Bawendi, Optical gain and stimulated emission in nanocrystal quantum dots, Science **290**, 314 (2000).

[66] A. J. Nozik, Spectroscopy and hot electron relaxation dynamics in semiconductor quantum wells and quantum dots, Annu. Rev. Phys. Chem. **52**, 193 (2001).

[67] N. Lenngren, M. A. Abdellah, K. Zheng, M. J. Al-Marri, D. Zigmantas, K. Žídek, and T. Pullerits, Hot electron and hole dynamics in thiol-capped CdSe quantum dots revealed by 2D electronic spectroscopy, Phys. Chem. Chem. Phys. **18**, 26199 (2016).

[68] L. Wang, Z. Chen, G. Liang, Y. Li, R. Lai, T. Ding, and K. Wu, Observation of a phonon bottleneck in copper-doped colloidal quantum dots, Nat. Commun. **10**, 4532 (2019).

[69] F. T. Rabouw, R. Vaxenburg, A. A. Bakulin, R. J. van Dijk-Moes, H. J. Bakker, A. Rodina, E. Lifshitz, A. L. Efros, A. F. Koenderink, and D. Vanmaekelbergh, Dynamics of intraband and interband Auger processes in colloidal core–shell quantum dots, ACS Nano **9**, 10366 (2015).

[70] K. Žídek, M. Abdellah, K. Zheng, and T. Pullerits, Electron relaxation in the CdSe quantum dot-ZnO composite: Prospects for photovoltaic applications, Sci. Rep. **4**, 7244 (2014).

[71] F. C. Spoor, S. Tomić, A. J. Houtepen, and L. D. Siebbeles, Broadband cooling spectra of hot electrons and holes in PbSe quantum dots, ACS Nano **11**, 6286 (2017).

[72] H. Haken, *Laser Light Dynamics* (North-Holland, Amsterdam, 1985), Vol. 2.

[73] M. O. Scully and S. Zubairy, *Quantum Optics* (Cambridge University, Cambridge, England, 1997).

[74] H. Carmichael, *An Open Systems Approach to Quantum Optics: Lectures Presented at the Université Libre de Bruxelles, October 28 to November 4, 1991* (Springer, Berlin, 2009), Vol. 18.

[75] W. Vogel and D.-G. Welsch, *Quantum Optics* (Wiley & Sons, New York, 2006).

[76] P. Kaer, N. Gregersen, and J. Mork, The role of phonon scattering in the indistinguishability of photons emitted from semiconductor cavity QED systems, New J. Phys. **15**, 035027 (2013).

[77] L. Wu, H. Wang, Q. Yang, Q.-x. Ji, B. Shen, C. Bao, M. Gao, and K. Vahala, Greater than one billion Q factor for on-chip microresonators, Opt. Lett. **45**, 5129 (2020).

[78] X. Cao, M. Zopf, and F. Ding, Telecom wavelength single photon sources, J. Semicond. **40**, 071901 (2019).

[79] X. He, H. Htoon, S. Doorn, W. Pernice, F. Pyatkov, R. Krupke, A. Jeantet, Y. Chassagneux, and C. Voisin, Carbon nanotubes as emerging quantum-light sources, Nat. Mater. **17**, 663 (2018).

[80] Ł. Dusanowski, C. Nawrath, S. L. Portalupi, M. Jetter, T. Huber, S. Klembt, P. Michler, and S. Höfling, Optical charge injection and coherent control of a quantum-dot spin-qubit emitting at telecom wavelengths, Nat. Commun. **13**, 748 (2022).

[81] R. J. Glauber, Optical coherence and photon statistics, in *Quantum Optics and Electronics*, edited by C. De Witt, A. Blandin, and C. Cohen-Tannoudji (Gordan and Breach, New York, 1965), p. 63.

[82] P.-A. Moreau, J. Mougin-Sisini, F. Devaux, and E. Lantz, Realization of the purely spatial Einstein-Podolsky-Rosen paradox in full-field images of spontaneous parametric down-conversion, Phys. Rev. A **86**, 010101(R) (2012).

[83] M. P. Edgar, D. S. Tasca, F. Izdebski, R. E. Warburton, J. Leach, M. Agnew, G. S. Buller, R. W. Boyd, and M. J. Padgett, Imaging high-dimensional spatial entanglement with a camera, Nat. Commun. **3**, 984 (2012).

[84] P. D. Blocher and K. Mølmer, Quantum regression theorem for out-of-time-ordered correlation functions, Phys. Rev. A **99**, 033816 (2019).

[85] I. V. Panyukov, V. Y. Shishkov, and E. S. Andrianov, Second-order autocorrelation function of spectrally filtered light from an incoherently pumped two-level system, Ann. Phys. **534**, 2100286 (2022).

[86] J.-H. Kim, S. Aghaeimeibodi, J. Carolan, D. Englund, and E. Waks, Hybrid integration methods for on-chip quantum photonics, Optica **7**, 291 (2020).

[87] S. Aghaeimeibodi, J.-H. Kim, C.-M. Lee, M. A. Buyukkaya, C. Richardson, and E. Waks, Silicon photonic add-drop filter for quantum emitters, Opt. Express **27**, 16882 (2019).

[88] R. M. Bakker, H.-K. Yuan, Z. Liu, V. P. Drachev, A. V. Kildishev, V. M. Shalaev, R. H. Pedersen, S. Gresillon, and A. Boltasseva, Enhanced localized fluorescence in plasmonic nanoantennae, Appl. Phys. Lett. **92**, 043101 (2008).

[89] G. Vecchi, V. Giannini, and J. Gómez Rivas, Shaping the Fluorescent Emission by Lattice Resonances in Plasmonic Crystals of Nanoantennas, Phys. Rev. Lett. **102**, 146807 (2009).

[90] T. Ming, H. Chen, R. Jiang, Q. Li, and J. Wang, Plasmon-controlled fluorescence: Beyond the intensity enhancement, J. Phys. Chem. Lett. **3**, 191 (2012).